ChemComm

COMMUNICATION

View Article Online
View Journal | View Issue

Cite this: *Chem. Commun.*, 2018, **54**, 2922

Received 26th January 2018,
Accepted 21st February 2018

DOI: 10.1039/c8cc00645h

rsc.li/chemcomm

Supramolecular self-assemblies for bacterial cell agglutination driven by directional charge-transfer interactions†

Dan Wu, *[a] Jie Shen,[b] Hongzhen Bai [a] and Guocan Yu[c]

Two supramolecular amphiphiles are fabricated through directional charge-transfer interactions, which self-assemble into nanofibers and nanoribbons. Due to the existence of galactose on their surface, these self-assemblies act as a cell glue to agglutinate *E. coli*, benefiting from multivalent interactions.

To develop ingenious self-assembly systems, such as supramolecular gels, supramolecular polymers, molecular machines and other multifunctional supramolecular systems, supramolecular chemistry is gaining extensive attention.[1] Lots of non-covalent interactions, like hydrophobic interaction, hydrogen bonding, π–π stacking interaction, charge-transfer interaction and electrostatic interaction, can be employed as driving forces to construct large supramolecular systems.[2] Supramolecular amphiphiles that are established by means of kinetic covalent bonds or non-covalent interactions have been applied in the construction of nanomaterials with a highly complex structure.[3] The emergence of supramolecular amphiphiles not only enlarges the scope of traditional amphiphiles, but also bridges the gap between supramolecular chemistry and colloidal science. In addition, with the help of a variety of non-covalent interactions, functional groups can be attached into the supramolecular amphiphiles more easily, providing a new approach for the preparation of well-defined nanostructures.[4]

Carbohydrates are one of the four fundamental biomacromolecules that also include nucleic acids, proteins and lipids, which play significant roles in biological activities and have already helped to develop new methods for the diagnosis and treatment of major diseases.[5,6] Due to the essential roles of carbohydrates in the regulation of various biological systems, great attention has already been paid to the construction of carbohydrate-based functional materials for studying carbohydrate–protein interactions.[7] Unfortunately, carbohydrate–protein interactions between monovalent carbohydrates and their putative receptors are always weak, usually only in millimolar levels. To circumvent this problem, multivalent interactions have been utilized to improve the binding efficiency.[8] Different from the stepwise polymerization process of peptides and oligonucleotides, the so complicated multivalent ligands are hardly synthesized by a conventional strategy.[9] Supramolecular self-assembly based on the non-covalent interactions is a useful technique to build such multivalent ligands, greatly reducing the need for a time-consuming chemical synthesis procedure.

Herein, we fabricated two supramolecular amphiphiles using three different bolaform amphiphiles as building blocks containing electron-rich naphthalene (**NP1** and **NP2**) or electron-deficient naphthalene diimide (**ND**) groups. Driven by the directional charge-transfer (CT) interactions, the formed X-shape (**NP1–ND**) and H-shape (**NP2–ND**) supramolecular amphiphiles self-assemble into one dimensional nanofibers and two dimensional nanoribbons, respectively. The galactoses as the hydrophilic groups on the surfaces of these self-assemblies serve as multivalent ligands to tightly bind with the receptors on *E. coli*, leading to remarkable cell agglutination.

Charge-transfer interactions between π-systems are important non-covalent interactions that have been greatly applied in the construction of supramolecular systems.[10] UV-Vis spectroscopy was first utilized to monitor the CT interactions between **NP1** and **ND**. When **NP1** and **ND** were simultaneously dissolved in water (molar ratio = 1 : 1), a characteristic CT band appeared, indicating the successful achievement of CT interactions (Fig. 1a).[11] Meanwhile, the mixed solution immediately turned plum, which is a characteristic color of naphthalene–naphthalene diimide CT complexes (Fig. 1a). As shown in Fig. 1b, the CT band corresponding to the complex enhanced dramatically by

[a] *Institute of Chemical Biology and Pharmaceutical Chemistry, Department of Chemistry, Zhejiang University, Hangzhou 310027, P. R. China. E-mail: 21106180@zju.edu.cn*
[b] *School of Medicine, Zhejiang University City College, Hangzhou 310015, P. R. China*
[c] *Laboratory of Molecular Imaging and Nanomedicine, National Institute of Biomedical Imaging and Bioengineering, National Institutes of Health, Bethesda, Maryland 20892, USA*

† Electronic supplementary information (ESI) available: ^{1}H NMR, UV-vis spectra, fluorescence emission spectra, concentration-dependent conductivity and scanning probe microscopy. See DOI: 10.1039/c8cc00645h

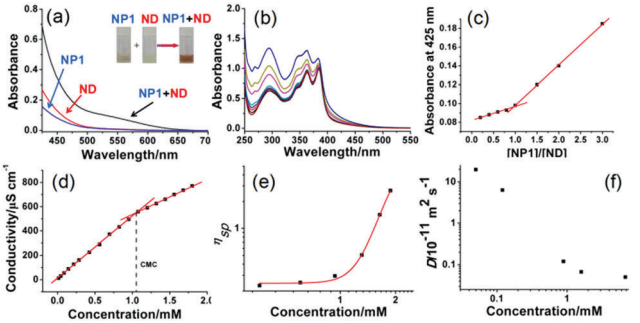

Fig. 1 (a) UV-Vis spectra of **NP1**, **ND** and mixture solution of **NP1** and **ND** (concentration: 2.50 × 10^{-4} M, molar ratio = 1 : 1). The inserted picture shows the color change of solution before and after complexation between **NP1** and **ND**. (b) UV-Vis titrations of **ND** (5.00 × 10^{-5} M) in water with various concentrations of **NP1** at room temperature: 0, 0.750, 1.50, 2.50, 3.75, 5.00, 7.50, 6.00, 10.0 and 15.0 × 10^{-5} M. (c) A mole ratio plot of the absorbance at 425 nm *versus* [**NP1**]/[**ND**] showing a 1 : 1 stoichiometry of the charge-transfer complex between **NP1** and **ND**. [**ND**] = 5.00 × 10^{-5} M. (d) The conductivities of **NP1–ND** at different concentrations. (e) Specific viscosity of the CT complex **NP1–ND** in water at room temperature *versus* the concentration of **NP1–ND**. (f) Concentration dependence of diffusion coefficient *D* of **NP1–ND** from the DLS results.

increasing the concentration of **NP1**, and a 1 : 1 stoichiometry between **NP1** and **ND** was confirmed by UV-Vis titration (Fig. 1c). In addition, fluorescence titration experiments were also employed to provide convincing evidence for the CT interactions. With the addition of **NP1**, the fluorescence intensity related to **ND** significantly decreased, indicating the formation of CT complexes (Fig. S5, ESI†).[12] On the other hand, CT interactions between the bolaform amphiphiles were further confirmed by ^{1}H NMR spectroscopy. As can be seen in Fig. S7 (ESI†), obvious changes in the chemical shift related to **NP1** could be observed after the addition of an equimolar amount of **ND** into the solution. The peaks related to protons a1, a2 and a3 on the naphthalene group of **NP1** underwent large chemical shift changes ($\Delta\delta$ = −0.34, −0.96 and −1.51 ppm for protons a1, a2 and a3, respectively), indicating that the protons on the naphthalene ring were situated at the center of the CT complex. It is worth mentioning that extensive broadening effects of the peaks related to the alkyl chains and naphthalene rings were observed due to the complexation dynamics. Considering that the size of naphthalene is smaller than that of naphthalene diimide, a face-centered packing mode (X-shape complex) is proposed (Scheme 1).[11a] Similar phenomena mentioned above were also observed between **NP2** and **ND** (Fig. S1–S4, S6 and S7, ESI†). Therefore, a reliable conclusion could be drawn that an H-shape complex was formed between the 2,6-substituted naphthalene **NP2** and **ND** groups. All these data indicated that CT interactions could be realized between electron-deficient naphthalene diimide units and electron-rich naphthalene groups, which was responsible for the formation of self-assembly nanostructures.

The concentration-dependent conductivity was applied to study the self-assembly behavior of CT complexes. As can be seen in Fig. 1d, the critical aggregation concentration (CAC) of **NP1–ND** (1.06 × 10^{-3} M) was obviously higher than those of **NP1** and **ND** (Fig. S8, ESI†). The reason was that the area of the

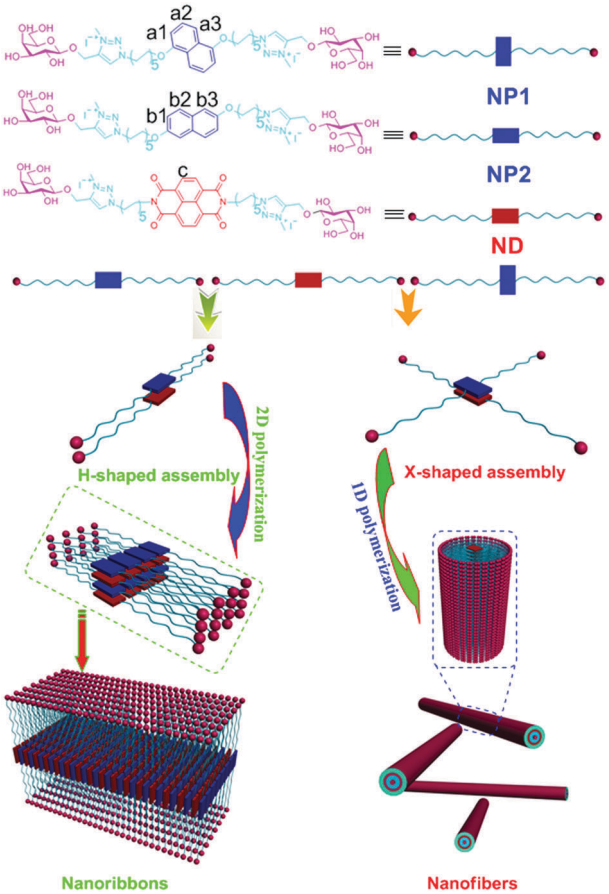

Scheme 1 Chemical structures of **ND**, **NP1** and **NP2** and schematic diagram of the self-assembly processes among **ND**, **NP1** and **NP2**.

hydrophobic parts decreased while the area of the hydrophilic parts increased accompanied by the formation of CT complexes, resulting in the change in their amphiphilicity. Microscopy observations indicated that the diameter and length of one dimensional nanofibers are about 7 nm and several micrometers (Fig. 2a). On account of the face-centered stacking mode between naphthalene diimide and naphthalene, which was greatly directional and perpendicular, the nanofibers were quite straight and smooth (Fig. 2b). The CAC value of H-shape complex **NP2–ND** was measured to be 1.36 × 10^{-3} M (Fig. S9b, ESI†), which was close to the CAC value of **NP1–ND**. Due to the different packing modes between **NP1–ND** and **NP2–ND** (Scheme 1), the nanostructures of the self-assemblies formed by **NP2–ND** were quite different from those of **NP1–ND**. Compared with the X-shape complexes, the H-shape complexes self-assembled into two dimensional nanoribbons about 20 nm in width and one micrometer in length (Fig. 2c and d). By using a scanning probe microscope, the thickness of the nanoribbons was measured to be about 7.4 nm (Fig. S10, ESI†). What calls for special attention is that the expanded length of the building blocks is about 6.1 nm, close to the thickness of the nanoribbons, indicating that the H-shape complex self-assembled into the nanoribbons in a single layer.

Interestingly, when the concentration of CT complexes was higher than 5.00 mM, the mobility of the solution decreased

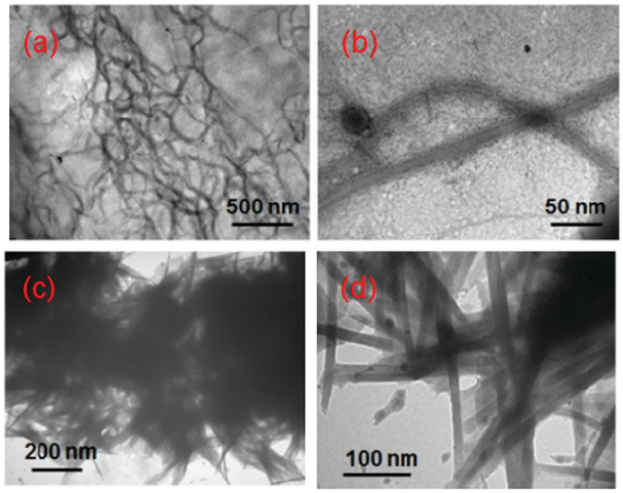

Fig. 2 (a) TEM image of the nanofibers self-assembled from **NP1–ND**. (b) Enlarged image of a. (c) TEM image of the nanoribbons self-assembled from **NP2–ND**. (d) Enlarged image of c.

rapidly. In order to further investigate their supramolecular aggregation in solution, the viscosities of the **NP1–ND** (or **NP2–ND**) solutions at different concentrations were measured using a Cannon-Ubbelohde semi-micro dilution viscometer. A double logarithmic plot of the specific viscosity *versus* concentration of monomer **NP1–ND** (or **NP2–ND**) was obtained. As shown in Fig. 1e and Fig. S11b (ESI†), the solution viscosity dramatically increased by increasing the CT complex concentration. The reason was that the X-shape complex of **NP1–ND** "polymerized" in one dimension to form thin and long nanofibers, and meanwhile the H-shape complex of **NP2–ND** "polymerized" in two dimensions to form high density nanoribbons.

The flow ability of the molecules of the solvent must be limited efficiently by the formation of nanofibers or nanoribbons, certainly leading to the rapid decrease of the diffusion coefficient (D).[13] The D value can be derived from the DLS results by using the Stokes–Einstein equation without any need to separate the species of mixtures. As shown in Fig. 1f, when the concentration of **NP1–ND** increased from 0.05 to 7.00 mM, the measured D value decreased dramatically from $(20.3 \pm 1.42) \times 10^{-11}$ to $(0.41 \pm 0.023) \times 10^{-12}$ m^2 s^{-1}, showing the concentration dependent behavior of the X-shape complex which underwent one dimensional "polymerization". Similarly, the D value related to the solution of **NP2–ND** also decreased significantly accompanying with the increase of the solution concentration due to the two dimensional "polymerization" of the H-shape complex (Fig. S11a, ESI†).

The simultaneous presentation of galactoses on the surfaces of the nanofiber/nanoribbon scaffolds provides a kind of polyvalent ligand that possesses a strong affinity to the carbohydrate receptors. For this reason, the multivalent carbohydrate-coated nanofibers/nanoribbons were employed as a competitive antibacterial agglutinant to suppress the growth of bacterial cells. In our previous work, we found that nearly no agglutinated *E. coli* cells with fluorescence could be observed after incubation with three bolaform amphiphiles (**ND**, **NP1** and **NP2**).[14] However, crowds of fluorescent bacteria were observed after *E. coli* were

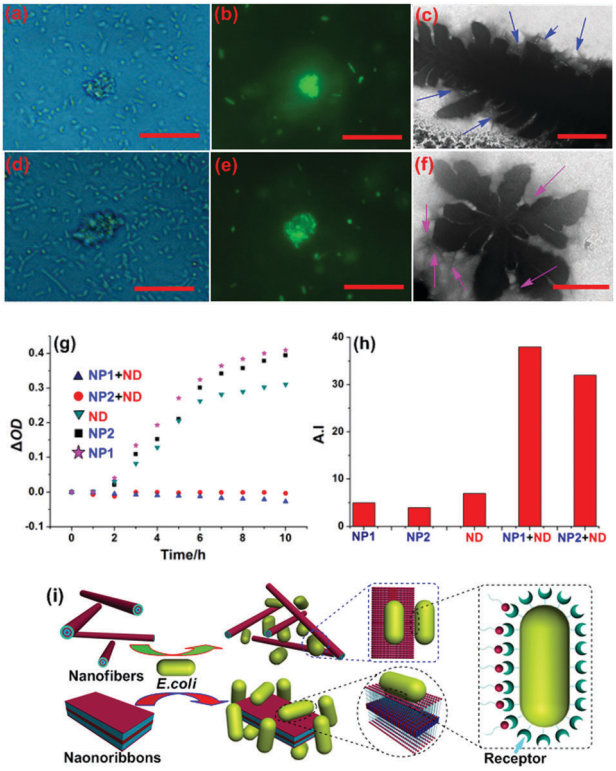

Fig. 3 (a) Optical microscopy image of **NP1–ND** (scale bar = 40 μm). (b) Fluorescence microscopy image of **NP1–ND** (λ_x = 360 nm, scale bar = 40 μm). (c) TEM image of **NP1–ND** (scale bar = 2 μm). (d) Optical microscopy image of **NP2–ND** (scale bar = 40 μm). (e) Fluorescence microscopy image of **NP2–ND** (λ_x = 360 nm, scale bar = 40 μm). (f) TEM image of **NP2–ND** (scale bar = 2 μm). (g) The growth curves of *E. coli* on the basis of optical density at 600 nm in the existence of **ND**, **NP1**, **NP2**, **NP1–ND** and **NP2–ND**. (h) Agglutination index acquired from TEM images and fluorescence microscopy. (i) Cartoon representation of *E. coli* agglutination in the existence of the nanofibers and nanoribbons.

incubated with galactose-coated nanofibers/nanoribbons for 10 h owing to their large size (Fig. 3b and e). TEM investigations also provided convincing evidence for the agglutination of *E. coli* cells induced by multivalent ligands on the surfaces of the nanofibers/nanoribbons (Fig. 3c and f, the nanofibers and nanoribbons are indicated by blue and purple arrows).

In order to fully investigate the inhibiting effect of the nanofibers/nanoribbons on the growth of *E. coli*, the bolaform amphiphiles and galactose-coated self-assemblies were added in an *E. coli* suspension, and the number variation of *E. coli* was monitored by optical microscopy. The variation of the optical density (ΔOD) in the suspension of *E. coli* after 1 h incubation was determined to reflect the number variation of the agglutinative *E. coli*. As shown in Fig. 3g, the cell population almost remained unchanged for **NP1–ND** and **NP2–ND** throughout the whole experiment, suggesting that the bacteria lost their motility and were completely inhibited by either the nanofibers or nanoribbons. According to the growth curves of **NP1–ND** and **NP2–ND**, the agglutination ability of **NP1–ND** was a little higher than that of **NP2–ND**. The reason was that the average length of the nanofibers could reach several micrometers, which was much greater

than that of the nanoribbons. In great contrast, **ND**, **NP1** and **NP2** containing divalent carbohydrates could not effectively bind their putative receptors on the surface of bacteria due to their low binding affinity. Furthermore, agglutination index (AI) analysis was conducted to evaluate the ability of bolaform amphiphiles and nanofibers/nanoribbons to agglutinate bacterial cells. As shown in Fig. 3h, the evaluated agglutination indexes corresponding to the nanofibers/naonoribbons were much higher than those of the bolaform amphiphiles (lower than 7), demonstrating the ability of the self-assemblies to aggregate *E. coli*.

In summary, two supramolecular amphiphiles (**NP1–ND** and **NP2–ND**) were obtained with the help of directional CT interactions between the electron-poor naphthalene diimide units and the electron-rich naphthalene moieties. Due to the different positions of substituted groups on the naphthalene groups of **NP1** and **NP2**, two distinct packing modes and self-assemblies were obtained. The X-shape complex corresponding to **NP1–ND** self-assembled into one dimensional nanofibers, while the H-shape complex related to **NP2–ND** formed two dimensional nanoribbons. Both of the self-assemblies were applied in *E. coli* cell agglutination due to the existence of abundant galactoses on the surfaces of the nanofibers/nanoribbons, which provided multivalent galactose ligands for putative receptors on bacterial cells. The nanofibers and nanoribbons acted as bridges to interconnect adjacent bacterial cells and their length played a crucial role in regulating the proliferation of bacterial cells. These biocompatible supramolecular self-assemblies with the ability to inhibit the growth of bacterial cells may also be a new bright star in other biology fields, such as targeted recognition/therapy, biological adhesives and so on.

This work was supported by the Fundamental Research Funds for the Central Universities.

Conflicts of interest

There are no conflicts to declare.

Notes and references

1 (*a*) J.-P. Collin, C. Dietrich-Buchecker, P. Gaviña, M. C. Jimene-Molero and J.-P. Sauvage, *Acc. Chem. Res.*, 2001, **34**, 477–487; (*b*) G. J. E. Davidson and S. J. Loeb, *Angew. Chem., Int. Ed.*, 2003, **42**, 74–77; (*c*) F. Huang and H. W. Gibson, *J. Am. Chem. Soc.*, 2004, **126**, 14738–14739; (*d*) S. Schlund, C. Schmuck and B. Engels, *J. Am. Chem. Soc.*, 2005, **127**, 11115–11124; (*e*) C. Wang, S. Yin, S. Chen, H. Xu, Z. Wang and X. Zhang, *Angew. Chem., Int. Ed.*, 2008, **47**, 9049–9052; (*f*) G. O. Lloyd and J. W. Steed, *Nat. Chem.*, 2009, **1**, 437–442; (*g*) W. Jiang, D. Sattler, K. Rissanen and C. A. Schalley, *Org. Lett.*, 2011, **13**, 4502–4505.

2 (*a*) Q.-C. Wang, D.-H. Qu, J. Ren, K. Chen and H. Tian, *Angew. Chem., Int. Ed.*, 2004, **43**, 2661–2665; (*b*) G. M. Pavan, A. Danani, S. Pricl and D. K. Smith, *J. Am. Chem. Soc.*, 2009, **131**, 9686–9694; (*c*) P. Wan, Y. Wang, Y. Jiang, H. Xu and X. Zhang, *Adv. Mater.*, 2009, **21**, 4362–4365; (*d*) W. Jiang, Q. Wang, I. Linder, F. Klautzsch and C. A. Schalley, *Chem. – Eur. J.*, 2011, **17**, 2344–2348; (*e*) D.-S. Guo, K. Wang, Y.-X. Wang and Y. Liu, *J. Am. Chem. Soc.*, 2012, **134**, 10244–10250; (*f*) A. Samanta, M. C. A. Stuart and B. J. Ravoo, *J. Am. Chem. Soc.*, 2012, **134**, 19909–19914.

3 (*a*) H. Ringsdorf, B. Schlarb and J. Venzmer, *Angew. Chem., Int. Ed.*, 1988, **27**, 113–158; (*b*) D. G. Bucknall and H. L. Anderson, *Science*, 2003, **302**, 1904–1905; (*c*) X.-Z. Zhu and C.-F. Chen, *J. Am. Chem. Soc.*, 2005, **127**, 13158–13159; (*d*) J.-H. Ryu, E. Lee, Y.-B. Lim and M. Lee, *J. Am. Chem. Soc.*, 2007, **129**, 4808–4814; (*e*) Y. Wang, H. Xu and X. Zhang, *Adv. Mater.*, 2009, **21**, 2849–2864.

4 (*a*) A. P. H. J. Schenning, J. V. Herrikhuyzen, P. Jonkheijm, Z. Chen, F. Würthner and E. W. Meijer, *J. Am. Chem. Soc.*, 2002, **124**, 10252–10253; (*b*) C. Park, J. Lim, M. Yun and C. Kim, *Angew. Chem., Int. Ed.*, 2008, **47**, 2959–2963; (*c*) C. Wang, Z. Wang and X. Zhang, *Acc. Chem. Res.*, 2012, **45**, 608–618; (*d*) G. Yu, C. Han, Z. Zhang, J. Chen, X. Yan, B. Zheng, S. Liu and F. Huang, *J. Am. Chem. Soc.*, 2012, **134**, 8711–8717; (*e*) S. Amemori, K. Kokado and K. Sada, *Angew. Chem., Int. Ed.*, 2013, **52**, 4174–4178.

5 (*a*) C. R. Bertozzi and L. L. Kiessling, *Science*, 2001, **291**, 2357–2364; (*b*) T. Angata and A. Varki, *Chem. Rev.*, 2002, **102**, 439–469.

6 (*a*) C. C. Lee, J. A. MacKay, J. M. J. Fréchet and F. C. Szoka, *Nat. Biotechnol.*, 2005, **23**, 1517–1526; (*b*) D. H. Dube and C. R. Bertozzi, *Nat. Rev. Drug Discovery*, 2005, **4**, 477–488; (*c*) F.-T. Liu and G. A. Rabinovich, *Nat. Rev. Cancer*, 2005, **5**, 29–41; (*d*) G. A. Rabinovich and M. A. Toscano, *Nat. Rev. Immunol.*, 2009, **9**, 338–352.

7 (*a*) P. R. Crocker, J. C. Paulson and A. Varki, *Nat. Rev. Immunol.*, 2007, **7**, 255–266; (*b*) S. J. Park, M.-R. Lee and I. Shin, *Chem. Soc. Rev.*, 2008, **37**, 1579–1591; (*c*) R. J. Pieters, *Org. Biomol. Chem.*, 2009, **7**, 2013–2025; (*d*) Q. Wu, L. Wang, H. Yu, J. Wang and Z. Chen, *Chem. Rev.*, 2011, **111**, 7855–7875; (*e*) Á. Martínez, C. O. Mellet and J. M. G. Fernández, *Chem. Soc. Rev.*, 2013, **42**, 4746–4773.

8 (*a*) R. Kikkeri, L. H. Hossain and P. H. Seeberger, *Chem. Commun.*, 2008, 2127–2129; (*b*) P. Wu, X. Chen, N. Hu, U. C. Tam, O. Blixt, A. Zettl and C. R. Bertozzi, *Angew. Chem., Int. Ed.*, 2008, **47**, 5022–5025; (*c*) D. Deniaud, K. Julienne and S. G. Gouin, *Org. Biomol. Chem.*, 2011, **9**, 966–979; (*d*) K.-R. Wang, H.-W. An, L. Wu, J.-C. Zhang and X.-L. Li, *Chem. Commun.*, 2012, **48**, 5644–5646; (*e*) K.-R. Wang, H.-W. An, Y.-Q. Wang, J.-C. Zhang and X.-L. Li, *Org. Biomol. Chem.*, 2013, **11**, 1007–1012; (*f*) T. R. Branson and W. B. Turnbull, *Chem. Soc. Rev.*, 2013, **42**, 4613–4622.

9 (*a*) M. K. Müller and L. Brunsveld, *Angew. Chem., Int. Ed.*, 2009, **48**, 2921–2924; (*b*) K. Petkau, A. Kaeser, I. Fischer, L. Brunsveld and A. P. H. J. Schenning, *J. Am. Chem. Soc.*, 2011, **133**, 17063–17071; (*c*) J. Hirabayashi, M. Yamada, A. Kuno and H. Tateno, *Chem. Soc. Rev.*, 2013, **42**, 4443–4458.

10 (*a*) Y. H. Ko, E. Kim, I. Hwang and K. Kim, *Chem. Commun.*, 2007, 1305–1315; (*b*) E. A. Appel, F. Biedermann, U. Rauwald, S. T. Jones, J. M. Zayed and O. A. Scherman, *J. Am. Chem. Soc.*, 2010, **132**, 14251–14260; (*c*) T. Xiao, X. Feng, S. Ye, Y. Guan, S.-L. Li, Q. Wang, Y. Ji, D. Zhu, X. Hu, C. Lin, Y. Pan and L. Wang, *Macromolecules*, 2012, **45**, 9585–9594.

11 (*a*) K. Liu, C. Wang, Z. Li and X. Zhang, *Angew. Chem., Int. Ed.*, 2011, **50**, 4952–4956; (*b*) K. Liu, Y. Yao, Y. Liu, C. Wang, Z. Li and X. Zhang, *Langmuir*, 2012, **28**, 10697–10702; (*c*) L. Yang, H. Yang, F. Li and X. Zhang, *Langmuir*, 2013, **29**, 12375–12379.

12 K. Liu, Y. Yao, C. Wang, Y. Liu, Z. Li and X. Zhang, *Chem. – Eur. J.*, 2012, **18**, 8622–8628.

13 S. Dong, Y. Luo, X. Yan, B. Zheng, X. Ding, Y. Yu, Z. Ma, Q. Zhao and F. Huang, *Angew. Chem., Int. Ed.*, 2011, **50**, 1905–1909.

14 G. Yu, J. Li, W. Yu, C. Han, Z. Mao, C. Gao and F. Huang, *Adv. Mater.*, 2013, **25**, 6373–6379.